Liquid Crystals
Publication details, including instructions for authors and subscription information:
http://www.informaworld.com/smpp/title~content=t713926090

Enhancing the electro-optical properties of ferroelectric liquid crystals by doping ferroelectric nanoparticles

Hao-Hsun Liang[a]; Ya-Zhi Xiao[a]; Fu-Jhen Hsh[a]; Che-Cheng Wu[a]; Jiunn-Yih Lee[a]
[a] Department of Polymer Engineering, National Taiwan University of Science and Technology, Taipei, Taiwan, Republic of China

Online publication date: 04 March 2010

To cite this Article Liang, Hao-Hsun , Xiao, Ya-Zhi , Hsh, Fu-Jhen , Wu, Che-Cheng and Lee, Jiunn-Yih(2010) 'Enhancing the electro-optical properties of ferroelectric liquid crystals by doping ferroelectric nanoparticles', Liquid Crystals, 37: 3, 255 — 261
To link to this Article: DOI: 10.1080/02678290903564403
URL: http://dx.doi.org/10.1080/02678290903564403

Liquid Crystals,
Vol. 37, No. 3, March 2010, 255–261

Taylor & Francis
Taylor & Francis Group

Enhancing the electro-optical properties of ferroelectric liquid crystals by doping ferroelectric nanoparticles

Hao-Hsun Liang*, Ya-Zhi Xiao, Fu-Jhen Hsh, Che-Cheng Wu and Jiunn-Yih Lee*

Department of Polymer Engineering, National Taiwan University of Science and Technology, Taipei 10607, Taiwan, Republic of China

(Received 27 April 2009; final version received 16 December 2009)

The effects on the physical and electro-optical properties of ferroelectric liquid crystals (FLCs) after the doping of a dilute suspension of ferroelectric nanoparticles ($BaTiO_3$) have been studied. Due to the permanent electric dipole moments of the ferroelectric nanoparticles, the spontaneous polarisation of FLCs with low doping concentration was about twice that of pure FLCs, in addition to a significant improvement in the dielectric properties, the response time and the V-shaped switching in the chiral smectic C (SmC*) phase. The results obtained point the way to an alternative for improving the applicability of FLCs without resorting to chemical synthesis.

Keywords: ferroelectric nanoparticles; ferroelectric liquid crystal; V-shaped switching; surface stabilised ferroelectric liquid crystal

1. Introduction

Recent studies of liquid crystals doped with nanoparticles have given rise to a number of novel practical applications [1] and pointed the way towards innovative improvement of the physical and electro-optical properties of liquid crystals by means of chemical synthesis.

Enhancement in the electro-optical properties of liquid crystals is dependent on the size, type, concentration and intrinsic characteristic of the nanoparticles used for doping. The nanoparticles should share similar attributes with the liquid crystal molecules and be of a size that would not cause serious disruption in the orderly arrangement of the liquid crystal. Low doping concentrations are usually chosen to yield a more stable and even distribution in the liquid crystal, which lowers the interaction forces between particles.

Commonly used doping nanoparticles include ferroelectric nanoparticles, ferromagnetic nanoparticles, metallic nanoparticles, inorganic nanoparticles, etc. Due to the large permanent dipole moments, ferroelectric nanoparticles induce realignment of neighbouring liquid crystal molecules, thereby increasing the order parameter and lowering the threshold voltage [2–6]. In the case of ferromagnetic nanoparticles, the large permanent magnetic moments induce changes in the ordering of the liquid crystal molecules, leading to improvements in the magnetic properties [7–11]. Under an electric field, the metallic nanoparticles give rise to a large Coulomb force and depolarisation, leading to enhancement in the memory effect of the liquid crystal [1, 12]. Inorganic nanoparticles, due to their intrinsic structures, can affect vertical alignment without the need for an alignment layer [13].

The discovery by Bachmann and Barner [14] that doping very fine dielectric particles into an isotropic liquid resulted in the enhancement of its sensitivity to electric fields heralded studies on the doping of ferroelectric nanoparticles ($BaTiO_3$, $Sn_2P_2S_6$) into nematic liquid crystals [15, 16]. In the beginning, the doping of nanoparticles was restricted to nematic liquid crystals due to their widespread applications and mature developments, as well as their relatively simple liquid crystal structure, which means that the doping of nanoparticles is less likely to destroy the alignment of the liquid crystal molecules. After the successful enhancement of the electro-optical properties of nematic liquid crystals, attention has been switched to other candidates for doping nanoparticles, such as cholesteric liquid crystals and smectic liquid crystals. After the doping of nanoparticles, there were significant improvements in the bi-stable states and driving voltage of the cholesteric liquid crystals. In the case of smectic A (SmA) liquid crystals, there were also significant improvements in the driving voltage [4].

In this study, we attempted to disperse ferroelectric $BaTiO_3$ nanoparticles after wet grinding into ferroelectric liquid crystals (FLCs) with a fast response time and a structure more complicated than nematic liquid crystals. We then infused a 2 μm liquid crystal cell to create a surface stabilised FLC (SSFLC) mode. Through measurements of the dielectric properties, spontaneous polarisation value, response time, V-shaped switching, etc. of the FLC, we attempted

*Corresponding authors. Email: jlee@mail.ntust.edu.tw; D9504402@mail.ntust.edu.tw

ISSN 0267-8292 print/ISSN 1366-5855 online

DOI: 10.1080/02678290903564403
http://www.informaworld.com

to improve its electro-optical properties through the large electric dipole moment of the low doping concentration $BaTiO_3$, without damaging the structure of the FLC.

2. Experiment

2.1 Materials

We made use of commercially available $BaTiO_3$ nanoparticles with an average size of 30–50 nm, polyhedron particle shapes (99+%, Aldrich), tetrahedral crystal structure, [001] polar axis and a spontaneous polarisation of 26 $\mu C\ cm^{-2}$ at room temperature. The dielectric constant of the $BaTiO_3$ single crystal is 168 in the direction parallel to the polar axis and 2920 in the direction perpendicular to the polar axis [17]. In contrast to other studies which used oleic acid as the surfactant and heptane as the solvent, we made use of a solution of polymeric dispersant (Just Nanotech) as the surfactant, taking advantage of the steric effect caused by the surfactant, where the polymer chains stick to the ferroelectric nanoparticles and thereby enhance the dispersion. For the solvent, we used tetrahydrofuran (THF). The phase transition temperatures of the FLC CS1024 (Chisso) we used are as follows:

$$\text{Crystal} \underset{-12^\circ C}{\longleftrightarrow} \text{SmC}^* \underset{62^\circ C}{\longleftrightarrow} \text{SmA} \underset{83^\circ C}{\longleftrightarrow} \text{N}* \underset{90^\circ C}{\longleftrightarrow} \text{Iso}$$

where SmC* represents the chiral smectic C phase, N* the chiral nematic phase and Iso the isotropic phase.

At 25°C, the spontaneous polarisation was –46.9 $nC\ cm^{-2}$, while the tilt angle was 25 degrees.

2.2 Sample preparation

We made use of a wet grinding dispersion equipment and yttria-stabilised zirconia (YSZ) as the grinding media. Commercially available ferroelectric $BaTiO_3$ nanoparticles, polymeric surfactant and THF were evenly mixed according to the weight ratio of 1:0.15:11. YSZ beads of the appropriate size were then chosen for 2 hours of wet grinding. After ultrasonic dispersion, the $BaTiO_3$ suspension was mixed with CS1024, and a vacuum was employed to evaporate the THF. After ultrasonic dispersion for an hour, we successfully prepared three samples with different doping concentrations: pure CS1024, CS1024 + 0.1 wt% susp. and CS1024 + 1 wt% susp. Thereafter, homogenous 2 μm (cell gap) cells were filled with pure FLCs or the FLC suspension at above the clearing temperature $T = 95^\circ C > T_c$. The cells consisted of two indium tin oxide (ITO)-coated glass substrates with a rubbed polyimide layer assembled for parallel alignment. The 2 μm rod-like glass spacers controlled cell spacing for producing the SSFLC mode.

2.3 Instruments

The dispersion was implemented with wet grinding dispersion equipment (Just Nanotech, JBM-B035). We made use of particle size analysers (PSAs, Brookhaven 90Plus/BI-MAS) and a transmission electron microscope (TEM, JEOL 2000FXII) for measurement of the size distribution of the $BaTiO_3$ nanoparticles, polarising optical microscopy (POM, OLYMPUS Optical Co., Ltd., Models BHSP-2, BX-51) for observing the liquid crystal phases, a differential scanning calorimeter (DSC, PerkinElmer PYRIS 1) for identification of the liquid crystal phase transition temperatures, and a low frequency impendence analyser (LFIA, Hewlett Packard 4192A) for measuring the dielectric properties. To determine the value of the spontaneous polarisation, we used the triangular wave measurements [18]. A He-Ne laser (632.8 nm, 10 mW) was employed as the light source, along with orthogonal polarisers, for measuring the response time and V-shaped switching characteristics.

3. Results

Before doping, the PSAs and TEM were used to determine the particle size distribution of the $BaTiO_3$ nanoparticles. After wet grinding to create the $BaTiO_3$ suspension, we added THF to yield a diluted 0.15 wt% $BaTiO_3$ suspension and performed particle size analysis with the dynamic light scattering technique. Figure 1 shows the results of the PSA measurement, with 99% of the $BaTiO_3$ particles having a size of less than 100 nm. The mean diameter was 39.9 nm. Figures 2(a) and (b)

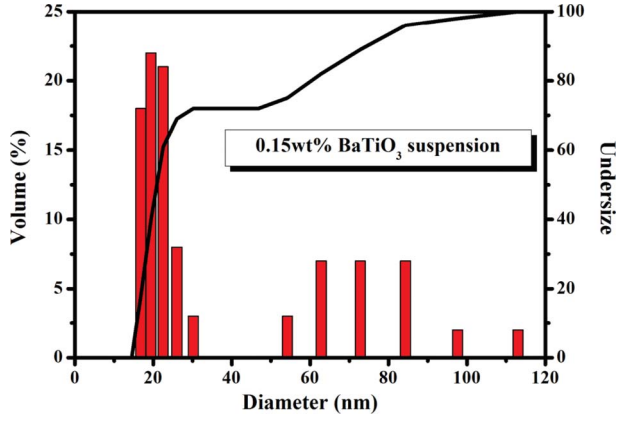

Figure 1. The results of the PSA measurement of 0.15 wt% $BaTiO_3$ suspension.

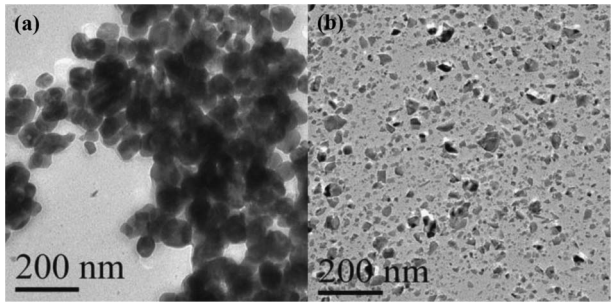

Figure 2. Transmission electron micrographs of $BaTiO_3$ nanoparticles (a) before and (b) after wet grinding.

show the TEM measurements before and after grinding. In Figure 2(a), the average $BaTiO_3$ particle size before grinding was about 90 nm, whereas in Figure 2(b), the average $BaTiO_3$ particle size after grinding was about 31 nm, indicating that the wet grinding and dispersion had successfully disrupted the aggregation of the nanoparticles, yielding an optimal nanoscale for ease of doping.

To ensure the rigor of the experiment, we first performed qualitative and quantitative analysis to ascertain that the composition of the FLC mixture CS1024 before and after vacuum treatment did not change [19]. The former involved the use of a Fourier transform infrared (FTIR) spectrometer (Digilab FTS-3500) and a mass spectrometer (Finnigan TSQ-700), whereas the latter made use of elemental analyser (HERAEUS VarioEL-III) measurements. The results of qualitative and quantitative analyses confirmed that the composition of the FLC mixture CS1024 was unchanged after vacuum treatment. Combining both the qualitative and quantitative analyses, we can conclude that the changes in the electro-optical properties were entirely the result of the contribution from the $BaTiO_3$ suspension and not due to changes in the composition of the CS1024 mixture during the preparation process.

The range of liquid crystal phase transition temperatures after doping was measured by POM and differential scanning calorimetry. Since the FLC material CS1024 is a compound, the phase transition temperature, unlike in single component liquid crystal material, is particularly hard to discern, particularly for the SmA and SmC* phase transitions. Table 1 shows the phase transition temperatures of FLCs with different doping concentrations. We can see that the Pure CS1024 and CS1024 + 0.1 wt% $BaTiO_3$ susp. had almost identical phase transition temperatures at $T_{N^*\text{-I}}$, $T_{N^*\text{-SmA}}$ and $T_{SmA\text{-}SmC^*}$, whereas there were slight decreases in the various phase transition temperatures of the CS1024 + 1 wt% $BaTiO_3$ susp. In particular, there was a decrease of about 4°C for the

Table 1. The phase transition temperature of CS1024 with different doping concentrations of $BaTiO_3$ suspensions.

Sample	Phase transition temperature
Pure CS1024	$SmC^* \overset{61.15^\circ C}{\longleftrightarrow} SmA \overset{82.58^\circ C}{\longleftrightarrow} N* \overset{90.35^\circ C}{\longleftrightarrow} Iso$
CS1024 + 0.1 wt% susp.	$SmC^* \overset{61.01^\circ C}{\longleftrightarrow} SmA \overset{82.35^\circ C}{\longleftrightarrow} N* \overset{90.12^\circ C}{\longleftrightarrow} Iso$
CS1024 + 1 wt% susp.	$SmC^* \overset{56.78^\circ C}{\longleftrightarrow} SmA \overset{81.89^\circ C}{\longleftrightarrow} N* \overset{89.68^\circ C}{\longleftrightarrow} Iso$

$T_{SmA\text{-}SmC^*}$ phase transition temperature. This result can alternatively be verified by measurements of the dielectric properties and spontaneous polarisation. After infusing the Pure CS1024 and the FLC suspension into a 2 μm liquid crystal cell to create a SSFLC mode, one can observe the texture of the higher doping concentration CS1024 + 1 wt% susp. under 200 times POM magnification (Figure 3). One can see clearly that there existed almost no characteristic texture of SmC*, indicating that we had successfully created a SSFLC mode. Other samples with different doping concentrations exhibited similar textures.

To investigate the effect of the doping concentration on the spontaneous polarisation, we adopted a two-pronged approach: varying the applied voltage at constant temperature and varying the temperature at the saturation voltage, using the triangular wave measurements for samples with different doping concentrations. Figure 4 shows the relation between the temperature and spontaneous polarisation for $BaTiO_3$ suspensions with different doping concentrations at $f = 10$ Hz and $V_{p\text{-}p} = 20$ V. The horizontal axis is the phase transition temperature from SmA to SmC* for samples with different doping concentrations and we can see that the spontaneous polarisation increased rapidly without reaching the maximum as the

Figure 3. The SSFLC texture of the CS1024 + 1 wt% susp. at 30°C under 200 times POM magnification. (The red arrow indicates the polyimide (PI) alignment rubbing direction. Colour refers to the online version.)

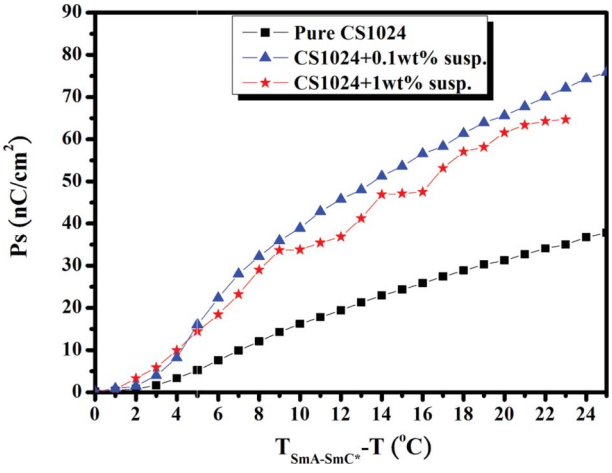

Figure 4. The dependence of the spontaneous polarisation for CS1024 with different doping concentrations of $BaTiO_3$ suspensions on the temperature at $f = 10$ Hz and $V_{p\text{-}p} = 20$ V.

temperature was cooled to the SmC* phase. In order to understand the sensitivity of the applied voltage to the doping concentration, we attempted to fix the temperature at 35°C in the SmC* liquid crystal phase, apply triangular waves with identical frequency ($f = 10$ Hz) but different voltages and observe the relation between the voltage and spontaneous polarisation for $BaTiO_3$ suspensions with different doping concentrations (Figure 5). We can see that other than a significant increase in the absolute values of the spontaneous polarisation, the p_s of the CS1024 + 0.1 wt% susp. (slope = 14.47099) and CS1024 + 1 wt% susp. (slope = 31.21684) also increased with the applied voltage. The slopes for the p_s values were also greater than those of Pure CS1024 (slope = 10.10697), further proof that the doping had significantly improved the sensitivity of the FLCs to an applied electrical field. In particular, the CS1024 + 0.1 wt% susp. exhibited the largest spontaneous polarisation, even reaching a value twice that of Pure CS1024 (80 nC cm^{-2}). Assuming that the p_s resulted from the contributions of the $BaTiO_3$ and FLCs, we can apply the zero order approximation to estimate the p_s value after doping:

$$P_s^{\text{susp.}} = (1 - f_w)P_s^{LC} + f_w P_s^{\text{particles}}, \qquad (1)$$

where f_w is the weight ratio of $BaTiO_3$ suspension. Using the above formula, one obtains a p_s value of about 68 nC cm^{-2} for the low doping concentration CS1024 + 0.1 wt% susp. and a p_s value of about 300 nC cm^{-2} for the high doping concentration CS1024 + 1 wt% susp., which is much higher than the experimental value of 65 nC cm^{-2}. One possible explanation for the discrepancy is that when interactions between the particles were ignored, the larger size of the nanoparticles compared to the liquid crystal molecules led to disruption of the FLC stacking, resulting in a smaller than expected p_s value.

For dielectric properties, Figure 6 shows the relation between the permittivity and temperature for the Pure CS1024, CS1024 + 0.1 wt% susp. and CS1024 + 1 wt% susp. at a frequency of 1 kHz. The permittivity increased drastically when cooling to 60°C in the SmC* phase. We can see from Figure 6 that there was little difference in the permittivity for the different liquid crystal phases of Pure CS1024 and CS1024 + 0.1 wt% susp., whereas the permittivity for the various liquid crystal phases of CS1024 + 1 wt% susp. was twice that of the others. In particular, the maximum permittivity of 42.9 occurred at 49°C, while the average permittivity of its SmC* phase was approximately 1.5 times that of the Pure CS1024 and CS1024 + 0.1 wt% susp. Therefore, one can see that the doping of $BaTiO_3$ will

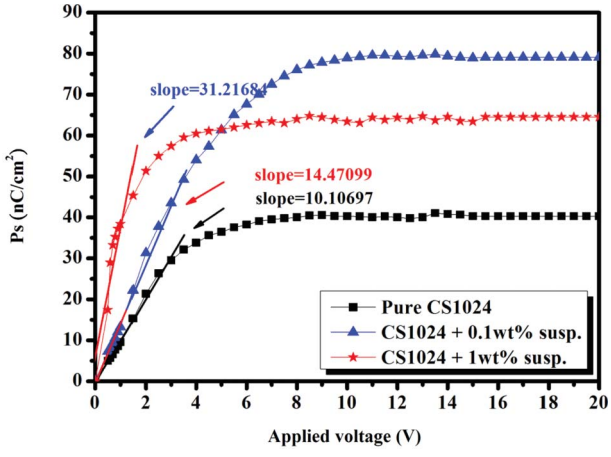

Figure 5. The dependence of the spontaneous polarisation for CS1024 with different doping concentrations of $BaTiO_3$ suspensions on the applied voltage at 35°C.

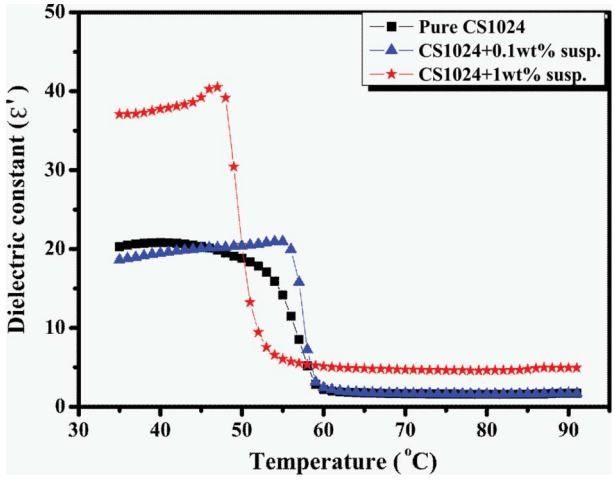

Figure 6. The dependence of the dielectric constant (ε′) for CS1024 with different doping concentrations of $BaTiO_3$ suspensions on the temperature at 1 kHz.

effectively enhance the permittivity of the liquid crystal material with its large electric dipole moment. In addition, one can also observe the significant differences in the slopes of the permittivity curves when the Pure CS1024, CS1024 + 0.1 wt% susp. and CS1024 + 1 wt% susp. samples entered the SmC* phase. A comparison of the Pure CS1024 and CS1024 + 0.1 wt% susp. revealed that while there was little difference between the permittivity, there was a very significant increase in the slope of the permittivity curve. The effect was especially prominent in the CS1024 + 1 wt% susp., thereby further affirming the observations on spontaneous polarisation. The doping of $BaTiO_3$ in liquid crystal material had enhanced its sensitivity to applied electric fields, and the permittivity curve exhibited a rapid increase on entering the SmC* phase before rising to the maximum value.

For the response time of the SSFLC mode, $V_{p\text{-}p} = 20$ V, $f = 10$ Hz was applied at a constant temperature of 35°C. Figure 7 shows the relation between the applied voltage and response time for the CS1024 + 0.1 wt% susp. One can see that the response time for the Pure CS1024, CS1024 + 0.1 wt% susp. and CS1024 + 1 wt% susp. decreased rapidly before saturating with increased applied voltage, evidence that the response time will saturate regardless of the applied voltage once the saturation voltage has been exceeded. Similar results were observed for the Pure CS1024 and CS1024 + 1 wt% susp. The response times for all three are tabulated in Table 2. The CS1024 + 1 wt% susp. had the minimum rise time and fall time, and listed in descending order of rise time and fall time values are the CS1024 + 1 wt% susp., Pure CS1024 and CS1024 + 0.1 wt% susp. The response time is the sum of the rise time and fall time, and assumed values

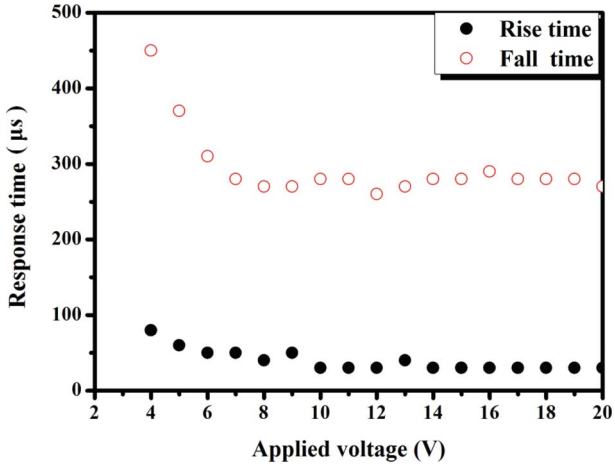

Figure 7. The dependence of the response time of CS1024 + 0.1 wt% susp. on the applied electric field.

Table 2. The response time of the SSFLC mode of CS1024 with different doping concentrations of $BaTiO_3$ suspensions.

Sample	Rise time (μs)	Fall time (μs)	Response time (μs)
Pure CS1024	75	360	435
CS1024 + 1 wt% susp.	30	280	310
CS1024 + 1 wt% susp.	100	370	470

of 435, 310 and 470 μs with increased doping concentrations. In addition,

$$\tau^{-1} \sim P_s \cdot {}^{E}/_{\gamma}, \tag{2}$$

where τ is the response time, γ is the intrinsic viscosity, p_s is the spontaneous polarisation and E is the electric field strength. We can infer that the CS1024 + 0.1 wt% susp., with a low doping concentration and the largest spontaneous polarisation under the same electric field, will have a shorter response time. On the other hand, while the spontaneous polarisation of the CS1024 + 1 wt% susp. was greater than that of Pure CS1024, the larger molecular weight of the polymeric surfactant in the suspension resulted in an overall increase in viscosity. The interplay of the two led to an increase in the response time. Taking into consideration the rise time and fall time performances of the different doping concentrations, we can conclude that the CS1024 + 0.1 wt% susp. is optimal.

The V-shaped switching of the SSFLC mode is shown in Figure 8, and we compared two scenarios: identical concentration but different frequencies and identical frequency but different concentrations. First of all, applying triangular waves of different frequencies at identical doping concentration, one can see that the hysteresis phenomenon became more pronounced with increasing frequency of the applied electric field (5–10 Hz), resulting in a pseudo W-shaped switching. Therefore, when the curve passed through the zero electric field, it was not possible to obtain a relatively dark state. There was also a phase shift in the relatively dark state, due to the fact that as the frequency of the applied electric field was increased, the liquid crystal molecules became unable to catch up with the switching frequency. On the other hand, for the V-shaped switching of triangular waves with identical frequency but different doping concentrations, the CS1024 + 0.1 wt% susp. exhibited the best V-shaped switching at 5 Hz, with no hysteresis phenomenon observable in the figure. The V-shaped switching properties of the CS1024 + 0.1 wt% susp. were superior to the Pure CS1024 at different frequencies, proving that doping $BaTiO_3$ resulted in enhancement of the V-shaped switching.

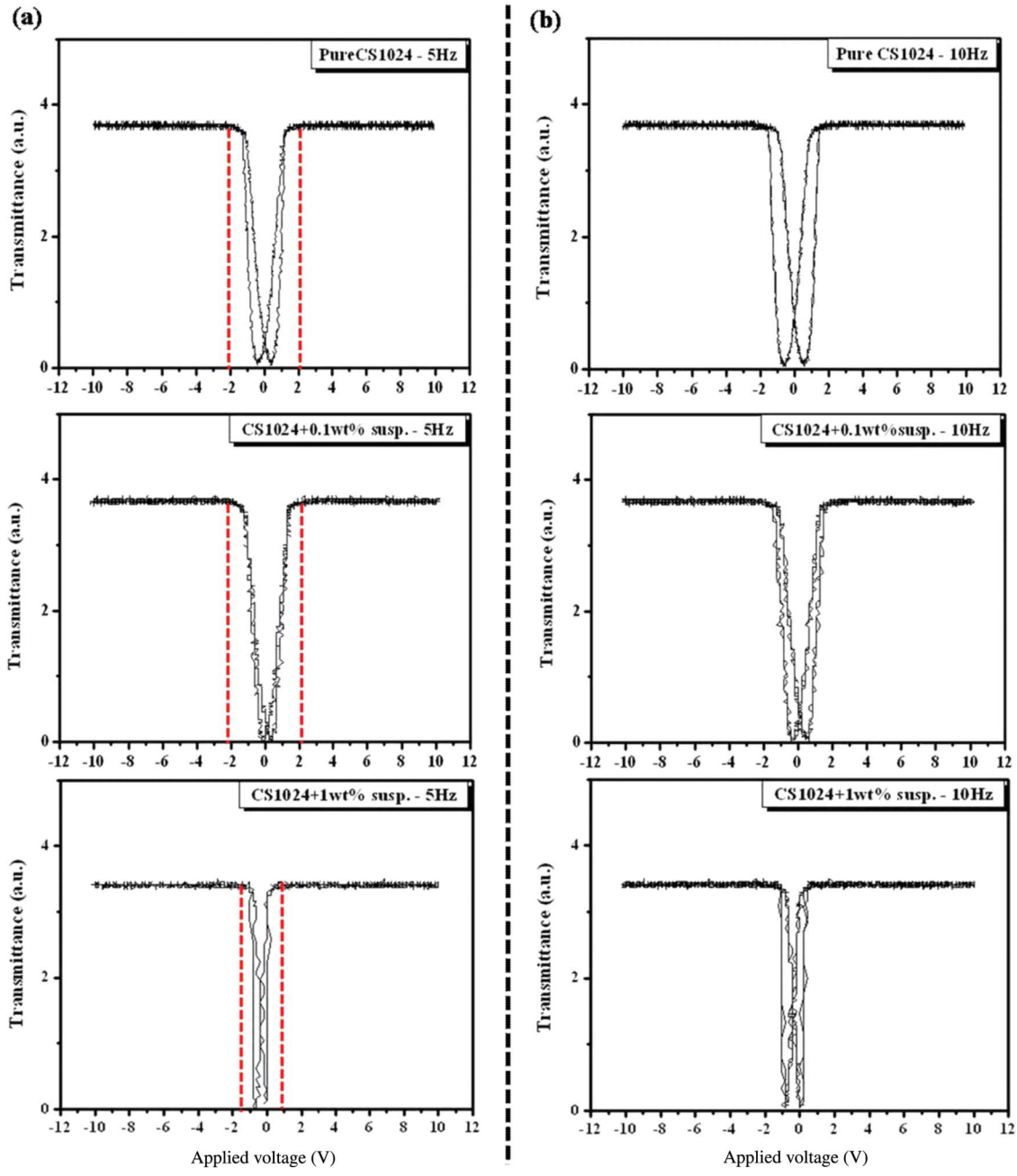

Figure 8. The dependence of the transmittance for CS1024 with different doping concentrations of $BaTiO_3$ suspensions on the applied triangular waveform voltage at (a) 5 Hz and (b) 10 Hz. (The red dashed line represents the switching between the two ferroelectric states. Colour refers to the online version.)

In particular, we examined in detail the case with the electric field at a frequency of 5 Hz and high doping concentration CS1024 + 1 wt% susp. We found that the greyscale performance was inferior to the Pure CS1024 and CS1024 + 0.1 wt% susp., but what was worth noting was that the voltage required for switching between the two ferroelectric states (the region demarcated by the red dashed line in the figure (colour refers to the online version)) was smaller than that for the Pure CS1024 and CS1024 + 0.1 wt% susp. From this phenomenon, we can indirectly infer that doping $BaTiO_3$ in the liquid crystal materials enhances its sensitivity to applied electric fields.

4. Conclusions

We have successfully dispersed commercially available $BaTiO_3$ nanoparticles into FLCs, drastically improving their electro-optical properties. Due to the large electric dipole moment of $BaTiO_3$, the spontaneous

polarisation of low doping concentration CS1024 + 0.1 wt% susp. was about twice that for Pure CS1024. There was also a significant improvement in the dielectric properties after doping, particularly in the SmC* phase. In both cases, increased sensitivity to application electric fields can be observed for the spontaneous polarisation and dielectric properties. The reproducibility of the results was confirmed after four months with the same experimental system and conditions. In addition, the CS1024 + 0.1 wt% susp. yielded the best V-shaped photoelectric switching and response time, pinpointing a way to improve the applicability of FLCs without resorting to chemical synthesis.

References

[1] Kobayashi, S.; Toshima, N. *Inf. Disp.* **2007**, *9/07*, 26–32.
[2] West, J.; Li, F.; Zhang, K.; Atkuri, H. *Proc. Asia Disp.* **2007**, *07*, 113–118.
[3] West, J.; Li, F.; Zhang, K.; Atkuri, H.; Glushenko, A. *Soc. Inf. Disp. Symposium Dig. Tech.* **2007**, *38*, 1090–1092.
[4] Glushchenko, A.; Cheon, C.; West, J.; Li, F.; Büyüktanir, E.; Reznikov, Y.; Buchnev, A. *Mol. Cryst. Liq. Cryst.* **2006**, *453*, 227–237.
[5] Reznikov, Yu.; Buchnev, O.; Tereshchenko, O.; Reshetnyak, V.; Glushchenko, A.; West, J. *Appl. Phys. Lett.* **2003**, *82*, 1917–1919.
[6] Li, F.; Buchnev, O.; Cheon, C.; Glushchenko, A.; Reshetnyak, V.; Reznikov, Y.; Sluckin, T.J.; West, J. *Phys. Rev. Lett.* **2006**, *97*, *147801-1-4*.
[7] Brochard, F.; de Gennes, P.G. *J. Phys. (Paris)*, **1970**, *31*, 691–708.
[8] Hayes, C.F. *Mol. Cryst. Liq. Cryst.* **1976**, *36*, 245–253.
[9] Chen, S.-H.; Nabil, M. *Phys. Rev. Lett.* **1983**, *51*, 2298–2301.
[10] Liang, B.J.; Chen, S.-H. *Phys. Rev.* **1989**, *A 39*, 1441–1446.
[11] Matuo, C.Y.; Figueriedo Neto, A.M. *Phys. Rev.* **1999**, *E 60*, 1815–1820.
[12] Kuar, S.; Singh, S.P.; Biadar, A.M.; Choudhary, A.; Sreenivas, K. *Appl. Phys. Lett.* **2007**, *91*, *023120-1-3*.
[13] Jeng, S.-C.; Kuo, C.-W.; Wang, H.-L.; Liao, C.C. *Appl. Phys. Lett.* **2007**, *91*, *061112-1-3*.
[14] Bachmann, R.; Barner, K. *Solid State Commun.* **1988**, *68*, 865–869.
[15] Cheon, C.; Li, L.; Glushenko, A.; West, J.; Reznikov, Y.; Kim, J.; Kim, D. *SID Symposium Dig. Tech.* **2005**, *36*, 1471–1473.
[16] Li, F.; West, J.; Glushchenko, A.; Cheon, C.; Reznikov, Y. *J. Soc. Inf. Disp.* **2006**, *14*, 523–527.
[17] Jaffe, B.; Cook, W.R.; Jaffe, H. Jr. *Piezoelectric Ceramics*; Academic Press Limited, 1971; pp49–55.
[18] Miyasato, K.; Abe, S.; Takezoe, H.; Fukuda, A.; Kuze, E. *Jpn. J. Appl. Phys.* **1983**, Tokyo, Japan, *22*, L661–663.
[19] Li, F.; Buchnev, O.; Cheon, C.; Glushchenko, A.; Reshetnyak, V.; Reznikov, Y.; Sluckin, T.J.; West, J. *Phys. Rev. Lett.* **2007**, *99*, 219901–1.